Short Communications

Contributions intended for publication under this heading should be expressly so marked; they should not exceed about 500 words; they should be forwarded in the usual way to the appropriate Co-editor; they will be published as speedily as possible; and proofs will not generally be submitted to authors. Publication will be quicker if the contributions are without illustrations.

Acta Cryst. (1955). **8**, 53

Two charts for setting the Buerger precession camera.†

By MURRAY VERNON KING, *The Protein Structure Project, Polytechnic Institute of Brooklyn, N.Y., U.S.A.*

(*Received 7 July and in revised form 18 August 1954*)

Two problems continually met in working with the Buerger precession camera are (i) the setting of the layer-line screen for isolation of a desired layer, and (ii) the reorientation of mis-set crystals by use of photographs taken without a layer-line screen. Two charts are given here for the rapid solution of these problems.

Alignment charts have been published by Evans, Tilden & Adams (1949) and by Tavora (1951) for use in setting the layer-line screen. However, the chart given here is of particularly simple form, and has been designed to be applicable to a wide range of radii of screens, including those which might be used in protein crystallography. Since the magnification factor F almost universally used is 60 mm., the $d^{*\prime}$ scale has been drawn for this value of F only.

The chart for setting the layer-line screen, Fig. 1, is

† Contribution No. 6 from The Protein Structure Project.

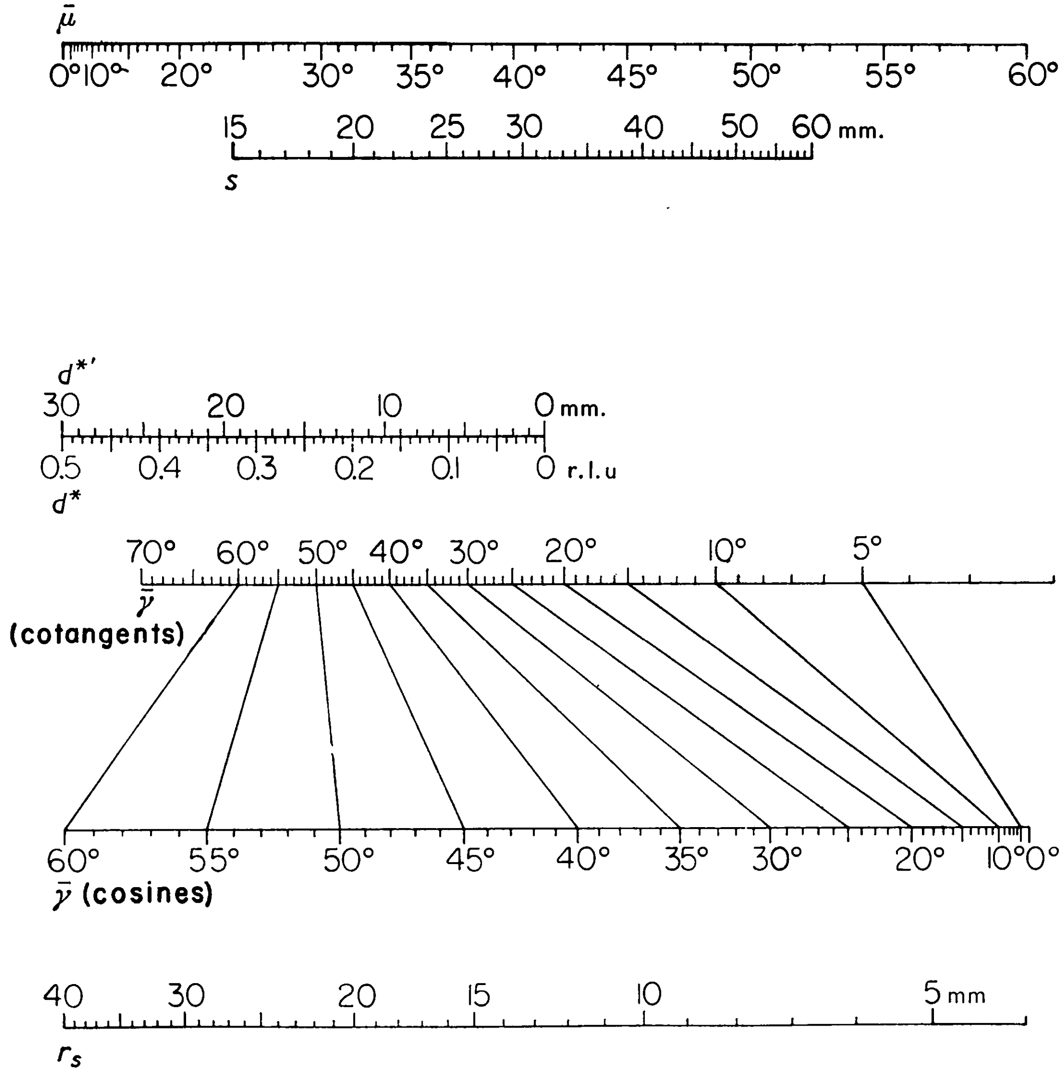

Fig. 1.

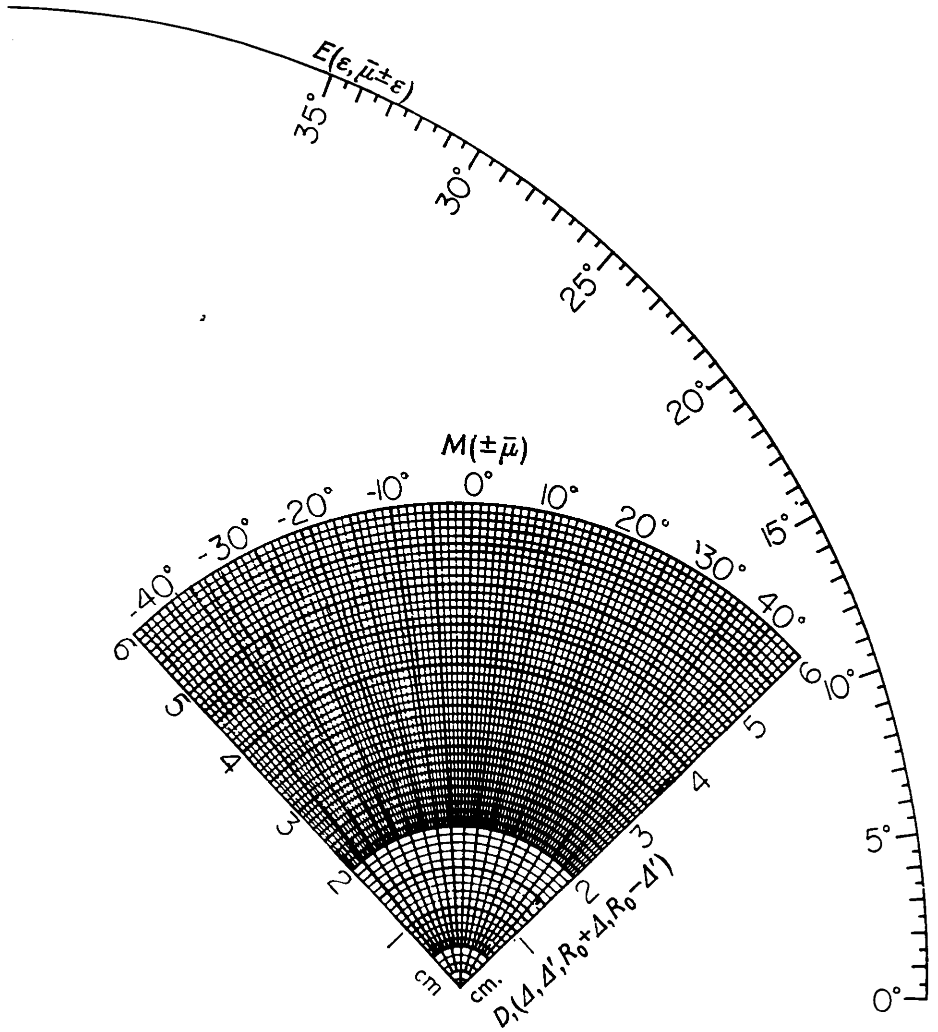

Fig. 2.

a combination of simple nomograms for solving the equations:

$$\cos \bar{\nu} = \cos \bar{\mu} - d^* ,$$

and

$$s = r_s \cot \bar{\nu} ,$$

where $\bar{\mu}$ is the precession angle, $\bar{\nu}$ is the cone angle of the desired layer, d^* $(= \lambda/d)$ is the height of this layer above the origin in reciprocal space, s is the crystal-to-screen distance, and r_s is the mean radius of the annular slit in the screen.

The chosen value of $\bar{\mu}$ and the required d^* are aligned with a ruler, and the value of $\bar{\nu}$ is read on the lower $\bar{\nu}$ (cosines) scale. This value is read off and found on the upper $\bar{\nu}$ (cotangents) scale; the point on the upper $\bar{\nu}$ scale is then aligned with an available screen radius r_s, and the corresponding value of s is read. If this value of s is not possible on the instrument, another value of r_s is tried.

The upper $\bar{\nu}$ scale has been extended to a value of 2° for convenience in screen settings for zero layers with very small values of $\bar{\mu}$. Such small values of $\bar{\mu}$ are often useful in recording the central area of the zero layer for crystals with large unit cells, and are sometimes necessary if the crystal is very small. When the chart is used for such zero-layer settings, inaccuracy due to the compression of the lower $\bar{\nu}$ scale at low values of $\bar{\nu}$ may be avoided, since $\bar{\nu} = \bar{\mu}$ for zero layers, and the value of $\bar{\mu}$ may be found directly on the upper $\bar{\nu}$ (cotangents) scale.

Fig. 1 may be used also to determine whether a given layer-line slit is sufficiently narrow to isolate a given nth layer from neighboring layers in reciprocal space. After r_s and s have been chosen for a given value of $\bar{\nu}$, the range of cone angles $\bar{\nu}$ which will pass through the slit is determined by connecting points $r_s + \frac{1}{2}w$ and $r_s - \frac{1}{2}w$ (w is the width of the slit) with the chosen value of s, and reading $\bar{\nu}$ on the upper scale. If this range does not include the cone angle values for the $(n+1)$th and $(n-1)$th layers, there will be no overlap of layers on the film. Obviously for any given slit width, the largest possible values of s and r_s will give the best resolution of layers.

The second chart, Fig. 2, is used to find the angle-of-orientation error ε of a crystal from the eccentricity of the observed area in which a central reciprocal-lattice plane records. Buerger (1944) has given an analytical method for finding ε from film measurements, the equations being based on the solution of triangles. The chart given here provides a simple graphical method for solving the triangles appearing in his method, but may also be used according to an alternative related method which is shorter.

A central reciprocal-lattice plane in its correct position parallel to the film will record within a circle of radius $FR = 2F \sin \bar{\mu}$. As Buerger has shown, when the reciprocal-lattice plane is inclined at an angle ε to the film, the margin of the area of recording is an eccentric curve. He denotes the maximum outward displacement of the margin beyond FR as $F\Delta$, and the maximum inward displacement as $F\Delta'$, and gives expressions for ε in terms of each.†

Fig. 3, reproduced from Buerger's monograph, shows that ε is obtained by solving triangle SUJ, with sides

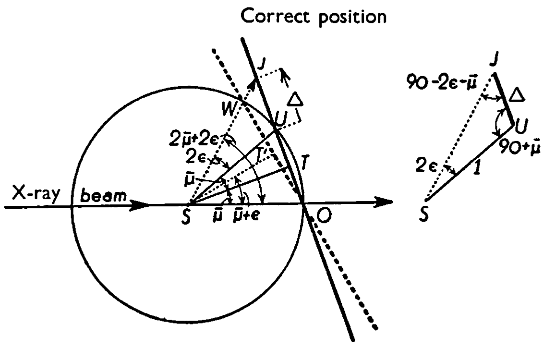

Fig. 3.

$SU = 1$, and $UJ = \Delta$, and $SUJ = 90° + \bar{\mu}$. The angle JSU is then 2ε. Similarly, 2ε may be obtained from a triangle of sides 1 and Δ', and included angle $90° - \bar{\mu}$.

The chart, Fig. 2, is a graph for rapid solution of a triangle with sides of lengths 1 and D and included angle $90° + M$. The coordinates on the D scale are multiplied by 60 for use with a camera with a magnification factor F of 60.‡ The angle opposite side D is designated as $2E$. The value of E is obtained by locating a point of coordinates (D, M) in the polar coordinate plot and aligning this point with the reference point in the lower left-hand corner. The ruler will intersect the E scale at the required value. Thus, ε may be obtained by alignment either with point $(F\Delta, \bar{\mu})$ or with point $(F\Delta', -\bar{\mu})$.

The procedure may be shortened, however. In order to find Δ or Δ' from film measurements, one must calculate $FR = 2F \sin \bar{\mu}$, and then find the displacements by difference. However, one may use directly the maximum radius, $F(R+\Delta)$, or minimum radius, $F(R-\Delta')$, of the area of recording. Thus, in Fig. 3, one may solve triangle SOJ, with sides $SO = 1$ and $OJ = R+\Delta$, and included angle $SOJ = 90° - \bar{\mu}$. The angle JSO is $2(\bar{\mu}+\varepsilon)$. Hence one may locate a point on Fig. 2 with $D = F(R+\Delta)$, $M = -\bar{\mu}$, and read $E = \bar{\mu}+\varepsilon$. Similarly, one may locate a point with $D = F(R-\Delta')$, $M = -\bar{\mu}$, and read $E = \bar{\mu}-\varepsilon$.

The modes of using Fig. 2 may be summarized thus:

Locate		Read
$D = F\Delta$	$M = \bar{\mu}$	$E = \varepsilon$
$D = F\Delta'$	$M = -\bar{\mu}$	$E = \varepsilon$
$D = F(R+\Delta)$	$M = -\bar{\mu}$	$E = \bar{\mu}+\varepsilon$
$D = F(R-\Delta')$	$M = -\bar{\mu}$	$E = \bar{\mu}-\varepsilon$

Charts are available from the Charles Supper Company, Newton Center, Mass., U.S.A., giving ε as a function of Δ for certain selected values of $\bar{\mu}$. While these charts are more accurate than Fig. 2, they are applicable only at the selected values of $\bar{\mu}$. Fig. 2 is applicable not only at intermediate values of $\bar{\mu}$, but also in cases where ε is very large, up to 35°. In practice, no difficulty arises when ε is greater than $\bar{\mu}$. In such cases, the area of recording has a blind space extending to one side from the origin, but Δ or Δ' may still be measured. Since Δ' then is greater than R, it is equal to R plus the *maximum* radius of the blind space.

The author wishes to thank Prof. M. J. Buerger for permission to republish Fig. 3, and Dr Thomas C. Furnas, Jr., and Miss Virginia Hong for assistance in preparation of the charts.

† It should be noted that some of Buerger's expressions are in error. Equation (25), p. 25 in his monograph, should read:

$$\cot 2\varepsilon = (1/\Delta) \sec \bar{\mu} + \tan \bar{\mu} .$$

Equation (23′), p. 25, should read:

$$\Delta' = \sin 2\varepsilon / \cos (2\varepsilon - \bar{\mu}) .$$

‡ Note that the D scale, as reproduced in Fig. 2, is not a scale of true centimetres.

References

Buerger, M. J. (1944). *The Photography of the Reciprocal Lattice*, pp. 21–6. ASXRED Monograph.

Evans, H. T., Jr., Tilden, S. G. & Adams, D. P. (1949). *Rev. Sci. Instrum.* **20**, 155.

Tavora, E. (1951). *An. Acad. Brasil Cienc.* **23**, 113.